Molecular Diffusion into Horse Spleen Ferritin: A Nitroxide Radical Spin Probe Study

Xiaoke Yang and N. Dennis Chasteen
Department of Chemistry, University of New Hampshire, Durham, New Hampshire 03824 USA

ABSTRACT Electron paramagnetic resonance spectroscopy and gel permeation chromatography were employed to study the molecular diffusion of a number of small nitroxide spin probes (~7–9 Å diameter) into the central cavity of the iron-storage protein ferritin. Charge and polarity of these radicals play a critical role in the diffusion process. The negatively charged radical 4-carboxy-2,2,6,6-tetramethylpiperidine-*N*-oxyl (4-carboxy-TEMPO) does not penetrate the cavity whereas the positively charged 4-amino-TEMPO and 3-(aminomethyl)-proxyl radical and polar 4-hydroxy-TEMPO radical do. Unlike the others, the apolar TEMPO radical does not enter the cavity but instead binds to ferritin, presumably at a hydrophobic region of the protein. The kinetic data indicate that diffusion is not purely passive, the driving force coming not only from the concentration gradient between the inside and outside of the protein but also from charge interactions between the diffusant and the protein. A model for diffusion is derived that describes the observed kinetics. First-order half-lives for diffusion into the protein of 21–26 min are observed, suggesting that reductant molecules with diameters considerably larger than ~9 Å would probably enter the protein cavity too slowly to mobilize iron efficiently by direct interaction with the mineral core.

Introduction

Ferritins are iron-storage proteins found in a variety of biological organisms, including vertebrates, invertebrates, plants, fungi, and bacteria (Theil, 1989; Harrison et al., 1991; Crichton, 1991; Proulx-Curry and Chasteen, 1995). Ferritins play an important role in the regulation of free iron within the cell. All ferritins are structurally very similar and are assembled from 24 polypeptide subunits to form a hollow spherical structure of 4:3:2 symmetry inside of which iron resides as a hydrous ferric oxide mineral (Harrison, 1959; Banyard et al., 1978; Ford et al., 1984; Harrison et al., 1985; Theil, 1987; Smith et al., 1989; Crichton, 1990). There are six hydrophobic channels along the fourfold axes and eight hydrophilic channels along the threefold axes leading to the inside of the protein (Rice et al., 1983; Ford et al., 1984; Harrison et al., 1986). It is believed that the threefold channels, which have a nominal diameter of 3–4 Å, constitute pathways through which iron and other molecular species gain access to the interior of the protein (Wardeska et al., 1986; Stefanini et al., 1989; Desideri et al., 1991, Treffry et al., 1993).

It has long been proposed that the mobilization of iron from the mineral core of ferritin involves the active participation of reductants and chelators (Jones et al., 1978; Crichton et al., 1975, 1980; Stefanini et al., 1975; Ford et al., 1984; Watt et al., 1985; Harrison et al., 1991). Whether such agents interact directly with the mineral core has been an important unresolved question in ferritin research. Many studies have been performed to determine the permeability of ferritin to reductants and to inert molecules of various sizes but with conflicting results (Stuhrmann et al., 1975; May and Fish, 1977; Jones et al., 1978; Watt et al., 1988; Jacobs et al., 1989; Webb et al., 1994). For example, diffusion studies have shown that [14C]glucose having a molecular cross section of ~7 Å slowly diffuses into the ferritin cavity over a period of several days whereas penetration does not occur with sucrose, which is approximately twice as big (May and Fish, 1977). However, these findings are in contradiction with neutron-scattering experiments that suggest that the diffusion of molecules such as glucose and sucrose into the ferritin cavity occurs within seconds (Stuhrmann et al., 1975, 1976). One study found that only free FMN can reduce the ferric core whereas FMN bound to a polymer cannot, a result implying that reductants must physically enter the ferritin cavity to react with the iron (Jones et al., 1978). However, other investigators found no evidence for the diffusion of FMN, methylviologen, and 2,2′-bipyridine into the ferritin cavity (Jacobs et al., 1989). Other studies support these findings by demonstrating that some reductants much larger than the ferritin channels are quite efficient at reducing the iron core provided their reduction potentials are low enough (Watt et al., 1988, 1992; Moore et al., 1992). Apparently, reductants need not necessarily enter the ferritin cavity to reduce the Fe(III). More recently, proton nuclear magnetic resonance relaxation data have been presented suggesting that molecules as large as maltose (13 Å) can penetrate the ferritin cavity in milliseconds (Yang and Nagayama, 1995). To explain why molecules much larger than the ferritin channels may be able to enter the cavity, a dynamic structural model in which subunits partially dissociate in dilute solution has been proposed (Massover, 1991, 1992, 1993).

The disparity in results regarding the size restrictions for molecular penetration into ferritin stems in part from ambiguity in the interpretation of previous data and from a lack

Received for publication 16 January 1996 and in final form 30 May 1996.
Address reprint requests to Dr. N. Dennis Chasteen, Department of Chemistry, Parsons Hall, University of New Hampshire, Durham, NH 03824-3595. Tel.: 603-862-2520; Fax: 603-862-4278; E-mail: ndc@christa.unh.edu.
© 1996 by the Biophysical Society
0006-3495/96/09/1587/09 $2.00

of direct kinetic measurements on the diffusion process itself. Such measurements are needed before one can confidently draw conclusions concerning the time scale, size restrictions, and pathways of molecular diffusion into ferritin. Nitroxide electron paramagnetic resonance (EPR) spin probes enable one to obtain these kinds of kinetics data.

Nitroxide radicals have been widely used as spin probes and labels in biological systems due to their relatively high chemical stability. EPR spectra yield valuable information about the microenvironment and mobility of nitroxide radicals (Berliner, 1976; Kocherginsky and Swartz, 1995). By choosing nitroxide spin probes with different charge and polarity, information about the charge interaction between the diffusant and the protein molecule can be revealed. Another advantage of using nitroxide spin probes as diffusants lies in the fact that the electron spin of the radical can interact with the superparamagnetic core of holoferritin leading to loss of the EPR signal of the radical as it gains access to the ferritin cavity. When the radical diffuses away from the iron core, the EPR signal is recovered. This phenomenon provides a convenient means to monitor the effusion of radicals from the ferritin interior.

The present study was undertaken to determine whether relatively small spin probe molecules of nominally ~7–9 Å cross section readily gain access to the ferritin cavity (as opposed to simply binding to the protein) and to measure the detailed kinetics of the process. By using EPR spin probes as diffusants in conjunction with gel permeation chromatography, one can establish whether the diffusant is bound to the surface of the protein, is detained in the channels, or ultimately gains access to the protein cavity. The data provide information about the kinetics and equilibrium of diffusion as well as the final destination of the diffusants.

Five nitroxide radicals were chosen for this study according to their charge and polarity. Among them, two are positively charged (I, II), one is polar (III), one is negatively charged (IV), and one is apolar (V) (Chart 1). The sizes of these five- and six-membered ring radicals are relatively the same, being nominally ~7–9 Å in diameter (Table 1).

MATERIALS AND METHODS

Materials

Cadmium-free horse spleen holoferritin was purchased from Boehringer Mannheim (Penzberg, Germany). The concentration of holoferritin was determined by using the Bio-Rad protein assay (Bio-Rad Laboratories, Hercules, CA) (Bradford, 1976; Sedmack and Grossberg, 1977). Horse spleen apoferritin was prepared by successive dialysis against dithionite and 2,2-dipyridyl under anaerobic conditions as described by Bauminger et al. (1991) and finally against 0.05 M 3-(*N*-morpholino)propanesulfonic acid (MOPS), 0.1 M NaCl, pH 7.5 buffer.

The nitroxide radical, 2,2,6,6-tetramethylpiperidine-*N*-oxyl (TEMPO), 4-amino-TEMPO, 4-carboxy-TEMPO, and Tb(III) chloride hexahydrate were purchased from Aldrich Chemical Co. (Milwaukee, WI), 3-(aminomethyl)-proxyl (3-aminomethyl-2,2,5,5-tetramethyl-1-pyrrolidinyloxy) and Sephadex G-25 from Sigma Chemical Co. (St. Louis, MO), and 4-hydroxy-TEMPO from Eastman Kodak Co. (Rochester, NY). MOPS (hemisodium salt) was manufactured by Research Organics (Cleveland, OH).

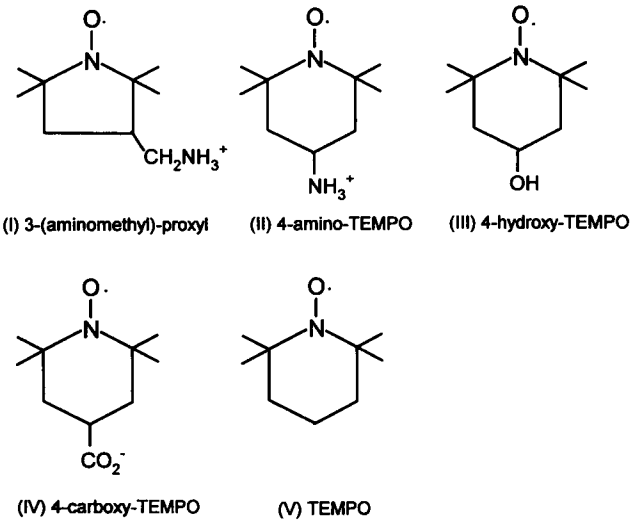

(I) 3-(aminomethyl)-proxyl (II) 4-amino-TEMPO (III) 4-hydroxy-TEMPO

(IV) 4-carboxy-TEMPO (V) TEMPO

Chart 1 Structures of the nitroxides at neutral pH.

The sizes of the nitroxide radicals indicated in Table 1 were determined with the computer program Spartan (Spartan Version 4.0.5, Wavefunction, 1995). After geometry optimization using the SYBYL force field, a space-filling model, Corey-Pauling-Kultun was used to portray the overall three-dimensional molecular size and the atomic radii chosen as approximating van der Waals contact distances.

Preparation of samples

Stock solutions of nitroxide radicals ranging from 20 to 140 mM, depending on their solubilities, were added to the holoferritin solution to reach final radical concentrations of 3 to 4 mM and a 24-mer protein concentration of approximately 0.1 mM. The sample was then incubated and aliquots were removed at various time intervals for chromatographic separation and EPR measurement.

To study the effect of Tb(III) binding on the rate of diffusion of the spin probe into the protein, the 0.1 mM holoferritin was first incubated with 3.0 mM terbium for 1 day and then with the 4.4 mM nitroxide radical for 70 min. To examine the effect of Tb(III) binding on the spin probe effusion process, holoferritin was first incubated with the nitroxide radical and then with Tb(III). Other treatments for these sample were the same as for samples without terbium.

Experimental set-up and method

The experimental procedure generally follows the pattern of incubation, separation, and measurement. A 1 × 15 cm Sephadex G-25 column equilibrated with 0.05 M MOPS buffer, 0.1 M NaCl, pH 7.5, was used to separate the protein from the free radical solutions. After separation, the protein fraction was measured by EPR spectroscopy to determine the radical concentration; the protein concentration was determined by using the Bio-Rad assay (Bradford, 1976; Sedmack and Grossberg, 1977). A home-assembled X-band EPR spectrometer consisting of a Bruker microwave bridge and field controller, an Alpha magnet and Varian magnet power supply, a PAR Lock-in amplifier, a Micro-Now field modulation amplifier, and a Varian TE_{104} rectangular cavity was employed to carry out the room temperature EPR measurements.

To decrease the time between the separation and EPR measurement, the Sephadex G-25 column was mounted directly on the EPR spectrometer. A quartz capillary with an inner diameter of 1 mm and outer diameter of 2 mm was connected to the outlet of the gel column and served as the EPR sample cell. In this way, the time dependence of the EPR signal of the protein fraction could be followed.

TABLE 1 Diffusion kinetic parameters for nitroxide radicals

Nitroxide radicals	Permeation process $k_1 \times 10^3$ (min^{-1})	Permeation process $k_{-1} \times 10^3$ (min^{-1})	Effusion process $k_{-1} \times 10^3$ (min^{-1})
4-Hydroxy-TEMPO 6.5 × 8.7 × 9.1 Å*	19.2 ± 2.5	27.0 ± 2.4	26.4 ± 0.8
4-Amino-TEMPO 6.6 × 8.9 × 9.1 Å*	27.5 ± 3.0	26.1 ± 1.3	23.2 ± 0.8
3-(Aminomethyl)-proxyl 7.0 × 7.1 × 8.4 Å*	33.3 ± 3.1	28.5 ±1.3	26.6 ± 0.8
TEMPO 6.5 × 8.1 × 8.9 Å*	Binds to protein		
4-Carboxy-TEMPO 6.6 × 9.1 × 9.9 Å*	No binding or permeation		

*The dimensions of the minimal sized rectangular box into which the molecule just fits are given (see Materials and Methods). The corresponding dimensions for glucose and $FMNH_2$ are 7.0 × 7.1 × 10.2 Å and 10.6 × 13.3 × 14.8 Å, respectively. The intermediate dimension of all of the molecules is the hypothetical molecular size limitation to penetration.

To monitor the permeation of the spin probe into the ferritin cavity, nitroxide-holoferritin samples were incubated for different times and separated on the column, and the protein fraction was aged for 24 h to allow the nitroxide radicals to diffuse out of the protein cavity completely. The EPR spectra of the protein samples were then taken and the concentrations of the radicals originally associated with the protein were determined by comparison with a nitroxide standard curve. The radical concentration inside the protein cavity, [A*], was determined from the relationship $[A^*] = f[A]_{meas}/q$, where f is the dilution factor from the chromatography step, q is the ratio of the total protein cavity volume to the solution volume (vide infra), and $[A]_{meas}$ is the measured radical concentration from the standard curve.

To study the effusion of the spin probe out of the ferritin cavity, holoferritin was first incubated with nitroxide radicals for approximately 2 h to achieve an equilibrium radical concentration inside the protein cavity. The sample was then loaded on the G-25 column and the elution stopped when the colored protein fraction was in the quartz capillary inside the EPR cavity. EPR measurements were started immediately, and repetitive scans were made with appropriate time intervals until the EPR amplitude of the liberated radical reached its maximal value.

Kinetic analysis

The permeation of small molecules into the ferritin cavity is a special case of a molecular diffusion process. The rate of the permeation is proportional to the molecular concentration outside the protein cavity, and the rate of the effusion is proportional to the molecular concentration inside the protein cavity. The diffusion driving force is simply the concentration difference between the outside and inside solutions. The overall process can be represented by the following simple equation:

$$A \underset{k_{-1}}{\overset{k_1}{\rightleftharpoons}} A^* \qquad (1)$$

where A represents a molecule outside the protein cavity and A* represents one inside the cavity. k_1 and k_{-1} are the rate constants for the permeation and effusion processes, respectively. It seems counterintuitive that the protein concentration would play no role in the rate of the diffusion process. However, an increase or decrease in the protein concentration does not produce any change in the radical concentration inside the protein cavity as a change in protein concentration also causes a corresponding change in the total protein cavity volume. In other words, the concentration of the radical inside the protein cavity is independent of the protein concentration and so must be the diffusion rate. The net rate of permeation into the protein cavity is given by

$$d[A^*]/dt = k_1[A] - k_{-1}[A^*], \qquad (2)$$

where [A*] and [A] represent the concentrations of A* and A, respectively, and $[A] = [A]_0 - q[A^*]$, $[A]_0$ being the initial concentration of A species and q being the ratio between the total protein cavity volume and the volume of the bulk solution. As the protein cavity volume is so small compared with the volume of the solution ($q \approx 10^{-2}$), [A] remains essentially a constant during the diffusion process, i.e., $[A] = [A]_0 = [A]_e$, where $[A]_e$ is the equilibrium concentration of A. Thus, diffusion into the protein under these conditions is a pseudo-zero-order process, and effusion from the protein is first-order. When Eq. 2 is integrated subject to the initial condition [A*] = 0 when $t = 0$, the first-order rate equation for the approach to equilibrium becomes

$$\ln(k_1[A]_0 - k_{-1}[A^*]) - \ln(k_1[A]_0) = -k_{-1}t. \qquad (3)$$

By using the relationship $[A^*]_e/[A]_e = k_1/k_{-1}$, Eq. 3 becomes

$$\ln([A^*]_e - [A^*]) - \ln[A^*]_e = -k_{-1}t. \qquad (4)$$

The slope of the logarithmic plot yields the negative value of the first-order effusion rate constant k_{-1}.

To obtain the permeation rate constant k_1, kinetic data from permeation measurements are fitted to a polynomial having the following form:

$$[A^*] = a + bt + ct^2 + dt^3, \qquad (5)$$

where t is the incubation time and a, b, c, and d are the fitting coefficients. The first derivative of Eq. 5 evaluated at $t = 0$ is equal to b, which is equivalent to $[A]_0k_1$.

For the effusion process, the initial concentration of the radicals inside the protein is $[A^*]_e$ and that of the radicals outside the protein is zero. As the total protein cavity volume is even smaller ($q < 10^{-3}$) compared with that for the permeation experiment, the increase in radical concentration outside the protein during the effusion is negligible so that the rate of diffusion back into the protein can be ignored. Thus, the rate of effusion can be represented as a simple first-order process:

$$d[A]/dt = k_{-1}q[A^*]. \qquad (6)$$

As $q[A^*]$ can be expressed as the difference between the equilibrium concentration of A and the concentration of A at diffusion time t, i.e., $q[A^*] = [A]_e - [A]$, Eq. 6 becomes

$$d[A]/dt = k_{-1}([A]_e - [A]). \qquad (7)$$

The integrated form is given by the following expression:

$$\ln([A]_e - [A]) - \ln[A]_e = -k_{-1}t \qquad (8)$$

Thus, first-order plots of both permeation data (Eq. 4) and effusion data (Eq. 8) yield independent values for k_{-1}. The equilibrium constant for the overall diffusion process is given by the ratio

$$K = k_1/k_{-1}. \qquad (9)$$

Results

The permeation process

Among the five nitroxide radicals tested, only the positively charged species (compounds I and II) and the polar species (compound III) were found to diffuse into the ferritin cavity. The negatively charged radical, 4-carboxy-TEMPO (compound IV) neither bound to the protein nor diffused into the

cavity under the same experimental conditions used for the other radicals. Unexpectedly, the apolar species, TEMPO (compound V) bound to the protein instead of diffusing into the protein cavity.

In a typical experiment, protein samples were incubated with the spin probe for different times. The protein was then rapidly separated on the gel column within 5 min and aged for 24 h to allow the radical to diffuse out of the protein, and the EPR spectrum of the liberated nitroxide was recorded. Spectra obtained for 3-(aminomethyl)-proxyl are shown in Fig. 1. The EPR amplitude increases with incubation time until a saturation value is reached, corresponding to the maximal concentration of the probe that had penetrated into the protein interior. The other two radicals, 4-amino-TEMPO and 4-hydroxy-TEMPO, show the same general behavior as that observed for 3-(aminomethyl)-proxyl (data not shown).

The concentrations of the nitroxides as a function of the incubation time are plotted in Fig. 2. Saturation is reached for the three radicals at approximately the same incubation time, but different saturation concentrations are achieved for each. The two positively charged radicals (compounds I and II) reached higher saturation concentrations than the polar radical (compound III). The concentrations correspond to an average of 0.39, 0.29, and 0.22 radicals per protein molecule for 3-(aminomethyl)-proxyl, 4-amino-TEMPO, and 4-hydroxy-TEMPO, respectively.

To investigate the pathway for diffusion into the protein, holoferritin was complexed with Tb(III), which is known to bind in the threefold channels at the three symmetry-related Asp-127 and the three Glu-130 residues (Treffry and Harrison, 1984; Harrison et al., 1986, 1990). Holoferritin samples, with and without Tb(III), were incubated with 3-(aminomethyl)-proxyl under identical conditions. The EPR spectra are shown in Fig. 3. At an incubation time of 70 min, the diffusion of the nitroxide into the protein was attenuated ~70% by the presence of Tb(III), a result implying that the threefold channels are the likely avenues by which the nitroxide radical gains access to the interior of the protein (see also below).

Based on the diffusion model (see Materials and Methods), the permeation of the nitroxide into ferritin can be treated as a first-order process regardless of the concentration of protein. The corresponding first-order plots are shown in Fig. 4. Because the rate of the permeation remains constant as the system approaches equilibrium under the experimental conditions employed, the slopes of the lines in Fig. 4 give only the effusion rate constant, k_{-1} (Eq. 4). To obtain the rate constant of the permeation process, the kinetic data are fitted to a third-order polynomial (Eq. 5); the permeation rate constant is determined by evaluating the first derivative of Eq. 5 at $t = 0$. The values of k_1 and k_{-1} determined from the permeation experiment are summarized in Table 1. Half-lives for permeation and effusion fall in the range 21–36 min.

The effusion process

The effusion of the nitroxide radical out of the ferritin cavity was conveniently monitored by the restoration of the EPR signal as the radical diffuses away from the magnetic core. Holoferritin was incubated with the radical for approximately 2 h to allow the latter to diffuse into the protein cavity and reach equilibrium. The sample was then separated on the gel column. Elution was stopped when the peak

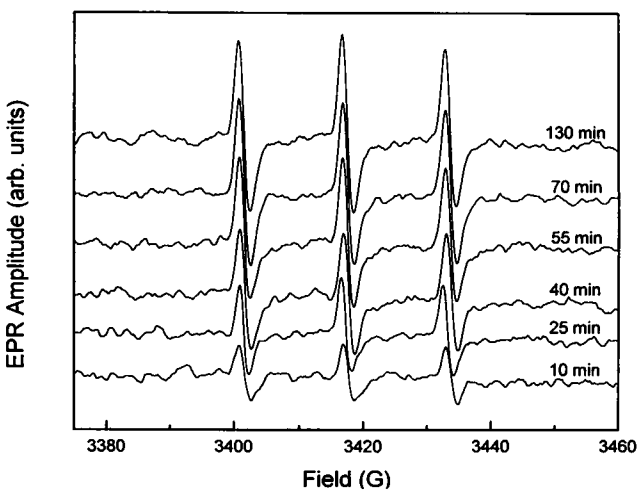

FIGURE 1 Time dependence of the room temperature EPR spectra for the diffusion of 3-(aminomethyl)-proxyl into holoferritin. The incubation time is indicated on each trace. Solution conditions for incubation were as follows: 0.117 mM holoferritin, 4.35 mM 4-hydroxy-TEMPO (data not shown), 3.75 mM 4-amino-TEMPO (data not shown), and 4.4 mM 3-(aminomethyl)-proxyl, pH 7.5. The dilution factor, f, from the chromatography step is ~15. Spectrometer settings were as follows: microwave power, 20 mW; frequency, 9.542 GHz; modulation amplitude, 1 G; time constant, 1 s; receiver gain, 1 mV.

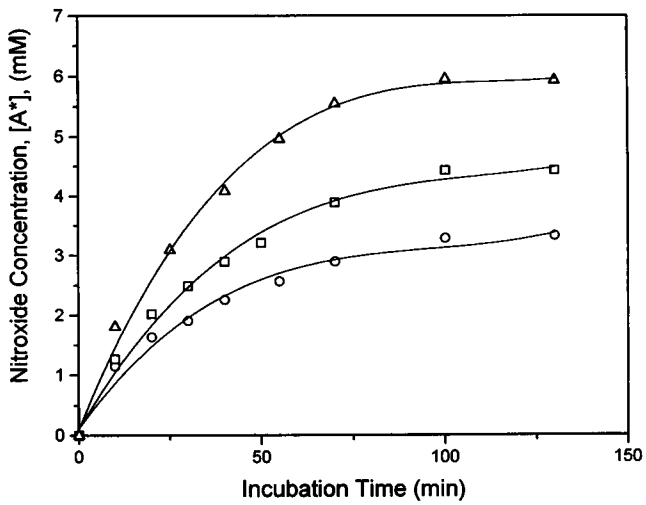

FIGURE 2 Time dependence of the concentrations of the nitroxides inside the protein cavity: 4-hydroxy-TEMPO (○), 4-amino-TEMPO (□), and 3-(aminomethyl)-proxyl (△). [A*] is determined from the relationship $[A^*] = f[A]_{meas}/q$ (see Materials and Methods). Solid lines are least-squares fits to Eq. 5.

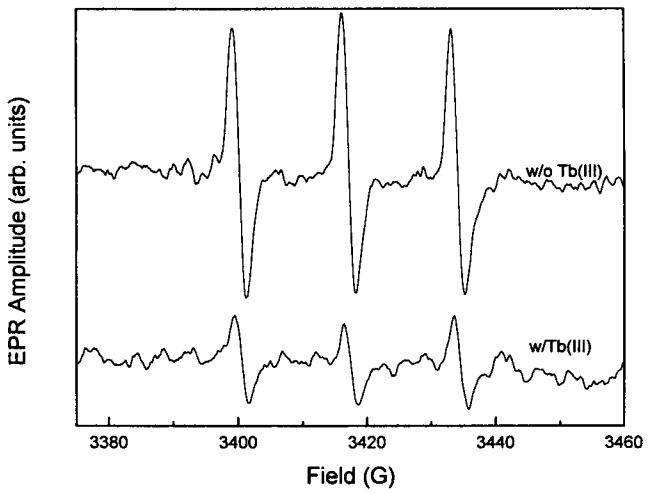

FIGURE 3 The effect of Tb(III) binding on the permeation of 3-(aminomethyl)-proxyl into holoferritin at room temperature. The incubation time for these measurements was 70 min. The top trace is protein without Tb(III). The bottom trace is protein with Tb(III). Solution conditions and spectrometer settings are the same as for Fig. 1.

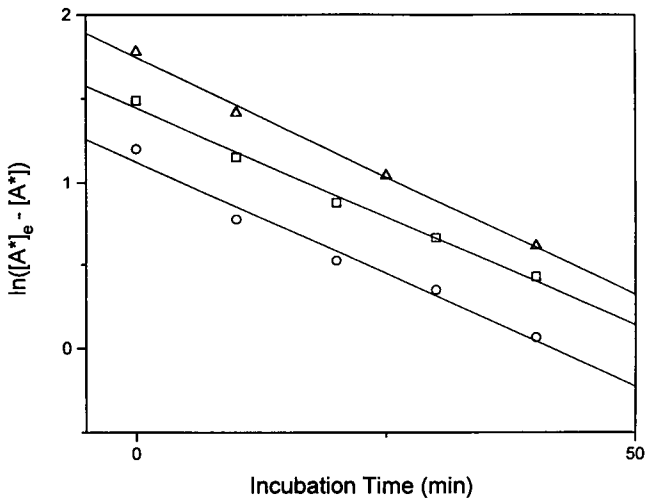

FIGURE 4 First-order plots for the permeation processes: 4-hydroxy-TEMPO (○), 4-amino-TEMPO (□), and 3-(aminomethyl)-proxyl (△).

concentration of the protein fraction reached the EPR cavity. Repetitive EPR scans were then started immediately and continued for several hours until no additional increase in the EPR amplitude was obtained. The time evolution of the EPR spectra for one of the radicals, 3-(aminomethyl)-proxyl, is given in Fig. 5 (for clarity, only some of the spectra are shown). Initially only a weak EPR signal was seen (bottom trace), which is due to the radical diffusing out of the protein during the 8-min time period required for the chromatographic separation plus EPR measurement. The signal increased as the radical continued to diffuse out of the protein cavity (Fig. 5).

The concentrations of the free radicals from diffusion out of the protein are plotted versus time in Fig. 6. The times for the concentrations of the two positively charged radicals to reach their final values are longer than for the permeation process, a result indicating a slower out pattern for these two radicals.

As the diffusion-in process can be ignored, the rate of the effusion from the protein is simply proportional to the concentration of the radical inside the protein. This concentration can be represented proportionally as the difference between the equilibrium concentration of the bulk solution at $t = \infty$ and its concentration at diffusion time t. The first-order plots for all three radicals are shown in Fig. 7, from which the rate constant k_{-1} for the effusion process is obtained directly from Eq. 8. The rate constants from the effusion measurements are also summarized in Table 1. The k_{-1} values obtained independently from the permeation and effusion experiments closely agree, validating the derived kinetic model for diffusion (see Materials and Methods).

The incubation time of holoferritin with the nitroxide, however, does influence the measured rate constant k_{-1} for effusion. For example, samples that had been incubated with the radicals for 1 week rather than 2 h yielded effusion rate constants k_{-1} approximately 50% as large as those in Table 1, a result indicating that, over the much longer incubation time, some additional association between the radical and the protein and/or mineral core occurs.

The effusion process was also examined with Tb(III)-complexed holoferritin samples to determine whether this process is also retarded by Tb(III). Samples of holoferritin, which had been previously incubated with the nitroxide, were incubated with 3.0 mM Tb(III). The increase in the EPR intensity with time after gel chromatography was then monitored. The rates of effusion of the radicals out of the Tb(III)-bound protein samples were approximately twofold slower compared with the unmodified samples (data not shown).

The equilibrium constant for the partitioning of the radicals between the interior and exterior of the ferritin can be

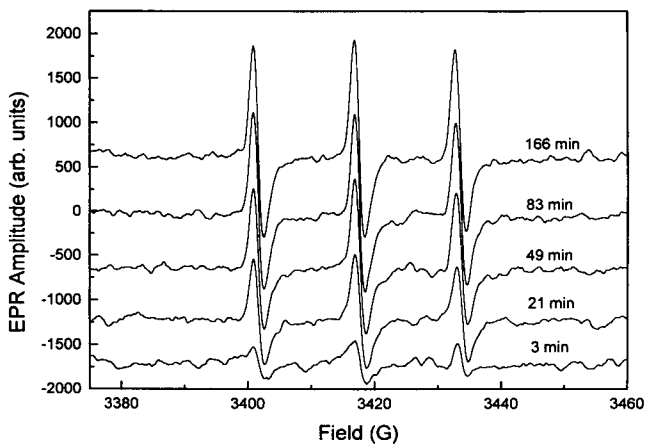

FIGURE 5 Time evolution of the EPR spectrum for the effusion of 3-(aminomethyl)-proxyl from holoferritin. The spectra were taken at room temperature. The effusion time is labeled on each trace. Solution conditions and spectrometer settings are the same as for Fig. 1.

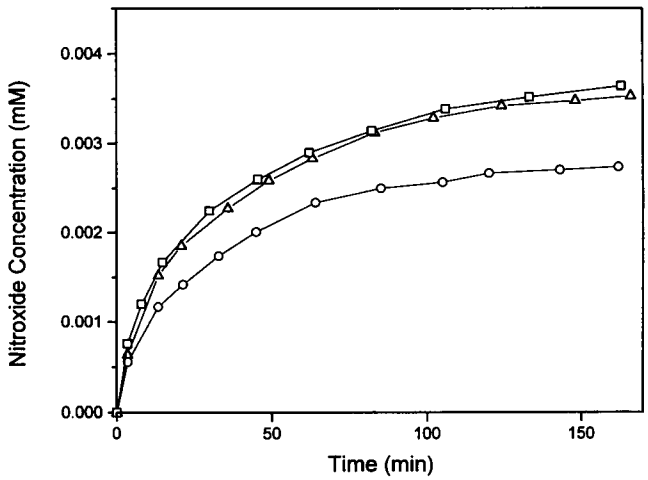

FIGURE 6 Time dependence of the concentrations for 4-hydroxy-TEMPO (○), 4-amino-TEMPO (□), and 3-(aminomethyl)-proxyl (△) effusion from holoferritin.

obtained by taking the ratio of the rate constants for the permeation and the effusion processes (Eq. 9). The equilibrium constant can also be calculated independently using the final equilibrium concentrations inside and outside the protein cavity. To determine the equilibrium concentration of the radicals inside the protein cavity, the free volume of the holoferritin cavity must be estimated. By using an inner diameter of 80 Å for the ferritin cavity (Ford et al., 1984), the free volume in the cavity is estimated to be 1.1×10^{-22} L, which is the volume occupied by the nitroxide radicals. This estimation is based on the density of the truncated hexagonal bipyramidal crystal of ferrihydrite given by Eggleton and Fitzpatrick (1988) and the 2200 Fe atoms per holoferritin used in this study. The computed equilibrium concentrations inside the protein based on this volume and the equilibrium constants from both the concentration and kinetic measurements are listed in Table 2. Good agreement between the values of K from the two methods is obtained, further confirming the validity of the kinetic and equilibrium analysis employed in this study.

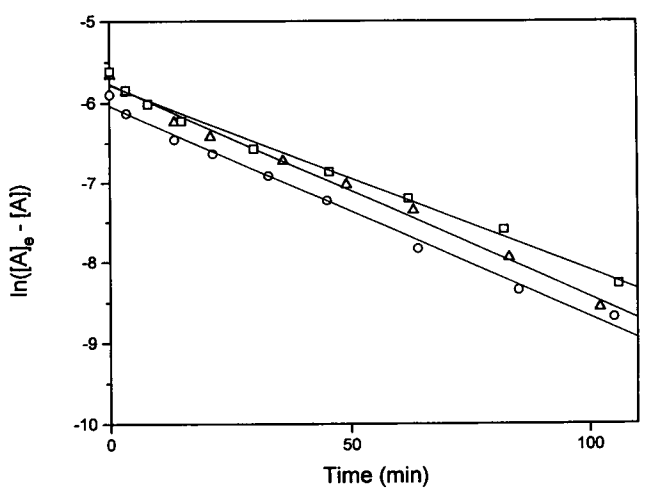

FIGURE 7 First-order plots for the effusion of 4-hydroxy-TEMPO (○), 4-amino-TEMPO (□), and 3-(aminomethyl)-proxyl (△) from holoferritin.

Binding of the apolar TEMPO radical to holoferritin

Unlike the other nitroxide radicals, the apolar radical TEMPO was found to bind to holoferritin. Immediately after the separation of the protein on the column, the EPR spectrum in Fig. 8 (lowest trace) is seen to be composed primarily of an immobilized component characteristic of a bound nitroxide (Desideri et al., 1991; Berliner, 1976) and a small sharp feature from free nitroxide. As shown in Fig. 8, the sharp component of the spectrum increases and the immobilized component decreases as the sample is aged, a phenomenon due to dissociation of the bound radical from the protein with a first-order half-life of 13 min. (The increase in intensity of the sharp feature is not due to effusion of the radical from the cavity as the total spectral EPR intensity as measured by double integration remains a constant as a function of time. If the radical had effused from the interior of the protein, an increase in the total EPR intensity would be expected.)

To further confirm that TEMPO does not diffuse into the protein cavity, control experiments were performed with apoferritin. As there is no iron core in apoferritin, any unbound radicals that had entered the cavity should produce a sharp EPR spectrum. However, the apoferritin sample after G-25 chromatography showed only the same immobilized TEMPO spectrum as that seen with holoferritin. The radical evidently binds exterior to the protein cavity in both apoferritin and holoferritin as the spectrum is not perturbed

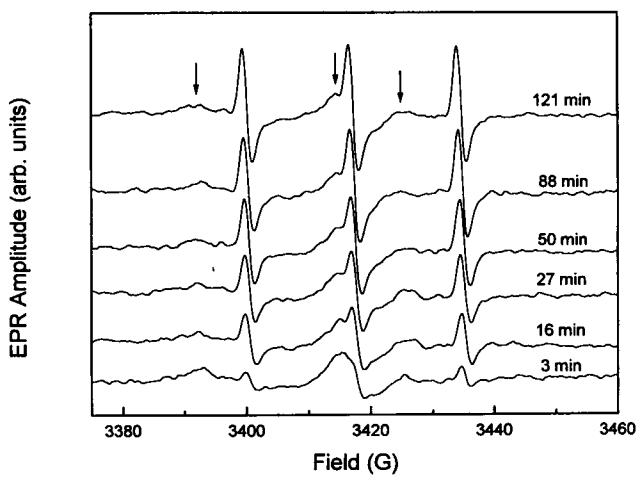

FIGURE 8 Time evolution of the EPR spectrum for the dissociation of TEMPO from holoferritin at room temperature. The dissociation time is indicated on each trace. The arrows denote spectral features from the immobilized component especially prominent in the 3-min spectrum. Solution conditions were as follows: 0.117 mM holoferritin and 3.0 mM TEMPO, pH 7.5. Spectrometer settings are the same as for Fig. 1, except receiver gain was 3 mV.

TABLE 2 Equilibrium parameters for the diffusion of nitroxide radicals into holoferritin

Nitroxide radicals	$[A]_e$ (mM)*	$[A^*]_e$ (mM)#	$K = [A^*]_e/[A]_e$§	$K = k_1/k_{-1}$¶
4-Hydroxy-TEMPO	4.35 ± 0.13	3.31 ± 0.10	0.761 ± 0.033	0.727 ± 0.147
4-Amino-TEMPO	3.75 ± 0.12	4.41 ± 0.14	1.18 ± 0.05	1.19 ± 0.13
3-(Aminomethyl)-proxyl	4.44 ± 0.14	5.93 ± 0.18	1.34 ±0.06	1.25 ± 0.10

*Determined from the EPR measurement.
#Calculated from EPR measurement and a protein cavity volume of 1.1×10^{-22} L.
§Equilibrium constant calculated from equilibrium concentrations.
¶Equilibrium constant calculated from diffusion rate constants using k_{-1} from the effusion experiment.

by the iron core. When the nitroxide apoferritin sample is subunit dissociated at pH 2, the immobilized component of the EPR spectrum disappears and the intensity of the sharp signal increases proportionately. This behavior suggests that the binding sites for TEMPO may be located at junctures between subunits, a likely candidate being the hydrophobic channels on the fourfold axes of the protein shell.

The other radicals were examined with apoferritin to determine whether they also bind to the protein. No evidence for binding was obtained. However, the two positively charged and the polar radicals elute with the apoprotein on size chromatography and exhibit EPR spectra characteristic of a freely tumbling spin probe molecule, indicating that they are trapped within the cavity but not bound to the protein itself as found for the holoferritin.

DISCUSSION

The permeability of ferritin to small molecules is an important property of the protein, enabling the deposition and mobilization of the iron core to occur. There is no question that the ferritin cavity is accessible to Fe^{2+}, O_2, H^+, OH^-, and H_2O. However, as noted in the Introduction, results from previous studies with larger molecular diffusants are not in uniform agreement due to very different experimental methods employed and to some ambiguity in interpretation of the data (May and Fish, 1977; Jones et al., 1978; Stuhrmann et al., 1975; Jacobs et al., 1989; Watt et al., 1988; Yang and Nagayama, 1995). Unlike previous approaches, the spectral properties of nitroxide spin probes allow us to directly study both structural and kinetic aspects of molecular diffusion into ferritin. For the first time, we have been able to establish the importance of charge and polarity of molecular diffusants on their ability to penetrate into the protein cavity, to determine the destination of diffusants in ferritin, to obtain rate information on the diffusion process, and to gain information on the mechanism and probable pathways of the diffusion.

The results show that only the positively charged and the polar radicals are able to diffuse into the protein cavity. The negatively charged and apolar species do not. Size is not a factor as all of the radicals are approximately the same size (~7–9 Å). Charge interactions undoubtedly play a role here, facilitating the entry of the positively charged radicals but inhibiting the negatively charged one. The failure of Fe^{3+}-chelating agents, which are generally negatively charged, to efficiently remove Fe^{3+} from the core of ferritin (Clegg et al., 1980) may well be due to the charge-selective properties of the protein observed here. This charge-selective behavior is consistent with the passing of small molecules down the hydrophilic threefold channels that are lined with negatively charged aspartate and glutamate residues (Ford et al., 1984; Harrison et al., 1990). The inhibition by Tb(III) of the rates of diffusion further supports the involvement of the threefold channels as avenues for molecular diffusion, although the postulated intra-subunit channel (Lawson et al., 1991) or other pathways are not precluded by the data.

The fact that the spin probes penetrate the protein despite their large size relative to the 3–4 Å diameter of the channels (Ford et al., 1984) indicates that there must be fluctuations from the static structure of the protein determined by x-ray crystallography. Such fluctuations probably account for the observation that protoporphyrin IX can penetrate along the twofold axis toward the inner surface of the protein shell as seen in the x-ray structure (Precigoux et al., 1994); however, the time scale for this process is unknown.

The failure of the negatively charged 4-carboxy-TEMPO radical to penetrate the protein does not preclude smaller anions such as Cl^-, OH^-, and HPO_4^{2-} from gaining access to the ferritin cavity, however. Experimental results show that chloride is transported into the cavity during the chemical reduction of the iron core by methylviologen (Hilty et al., 1994). In the special case of OH^-, H^+ ion is generated in the interior of the ferritin during Fe(III) hydrolysis to form FeOOH with charge compensation being achieved by the H^+ ion diffusion out of the cavity (Chen-Barrett, 1994). Phosphate is a well known constituent of the cores of various ferritins (Proulx-Curry and Chasteen, 1995) and thus must freely gain access to the protein interior as well. The molecular anion dithionite $S_2O_4^{2-}$ or its radical $SO_2^{\cdot -}$, commonly employed to reduce the core, probably penetrates the protein cavity also, although its negative charge makes it a less effective reducing agent than cationic methylviologen (Jacobs et al., 1989). Reduction of the core can occur without penetration as has been demonstrated with large molecular weight reductants (Watt et al., 1988).

The kinetics data in Table 1 indicate that permeation of the spin probes into the ferritin cavity is relatively fast ($t_{1/2} \approx$ 21–26 min) compared with the early studies of glucose by May and Fish (1977) ($t_{1/2}$ on the order of days) and much slower than the rates concluded from the neutron-scattering studies (Stuhrmann et al., 1975, 1976)

($t_{1/2}$ on the order of seconds). The present results are also at variance with the rapid rates ($t_{1/2}$ on the order of milliseconds) concluded from recent nuclear magnetic resonance data, the analysis of which requires a number of assumptions (Yang and Nagayama, 1995). In contrast to these previous studies, the exchange rates have been measured directly in the present work. The validity of the analysis is demonstrated by the independent determination of effusion and permeation rates (Table 1) and by the self-consistency in equilibrium constants derived independently from kinetics and concentration measurements (Table 2). Thus, from our data we conclude that the diffusion of moderately sized molecules into ferritin is a relatively slow process and reducing agents as large as FMN or other flavins are unlikely to gain access to the interior of ferritin at rates that are sufficiently fast to mobilize iron by direct interaction with the core. Electron transfer across the protein shell as originally postulated by Watt and co-workers (1988) seems the more likely mechanism for Fe(III) reduction involving large flavin molecules.

It is significant that the positively charged nitroxide radicals have equilibrium constants greater than 1, due to faster rates of diffusion into the protein than out (Tables 1 and 2), indicating that there is a weak association between the positively charged nitroxides and the ferritin cavity. These interactions perhaps involve the core or the numerous carboxylate groups lining the inside surface of the protein cavity (Ford et al., 1984; Harrison et al., 1990). In the case of 4-hydroxy-TEMPO, an equilibrium constant less than unity is observed because of its slower rate of diffusion into the protein. From these observations and analysis, it is clear that purely passive diffusion does not occur for any of the radicals. For pure passive diffusion, k_1 and k_{-1} should be the same with an equilibrium constant of unity. The driving force for diffusion into holoferritin is not only the concentration gradient but also the attractive interaction between the protein and the charged radicals. Such interactions are probably a central feature of the ion exchange properties of the ferritin core, accounting for its ability to bind a variety of cations (Price and Joshi, 1983; Fleming and Joshi, 1987).

This study was supported by USPHS grant R37 GM20194 (N. D. Chasteen) from the National Institute of General Medical Sciences.

REFERENCES

Banyard, S. H., D. K. Stammers, and P. M. Harrison. 1978. Electron density map of apoferritin at 2.8 Å resolution. *Nature.* 271:282–284.

Bauminger, E. R., P. M. Harrison, D. Hechel, I. Nowik, and A. Treffry. 1991. Mossbauer spectroscopic investigation of structure-function relations in ferritins. *BBA.* 1118:48–58.

Berliner, L. J. 1976. Spin Labels, Theory and Applications. Academic Press, New York.

Bradford, M. 1976. A rapid and sensitive method for the quantitation of microgram quantities of protein utilizing the principle of protein-dye binding. *Anal. Biochem.* 72:248–254.

Chen-Barret, Y. 1994. Characterization of radical formation and iron oxidation/hydrolysis during iron deposition in ferritin. Ph.D. thesis, University of New Hampshire, Durham, NH, 176 pp.

Clegg, G. A., J. E. Fitton, P. M. Harrison, and A. Treffry. 1980. Ferritin: molecular structure and iron-storage mechanisms. *Prog. Biophys. Mol. Biol.* 36:1–34.

Crichton, R. R. 1990. Proteins of iron storage and transport. *Adv. Protein Chem.* 40:281–363.

Crichton, R. R. 1991. Inorganic Biochemistry of Iron Metabolism. Ellis Horwood, New York.

Crichton, R. R., F. Roman, F. Roland, E. Paques, A. Paques, and E. Vandamme. 1980. Ferritin iron deposition and mobilization. *J. Mol. Catal.* 7:267–276.

Crichton, R. R., M. Wauters, and F. Roman. 1975. Ferritin iron uptake and release. *In* Proteins of Iron Storage and Transport in Biochemistry and Medicine. R. R. Crichton, editor. North Holland/Elsevier, Amsterdam. 287–294.

Desideri, A., S. Stefanini, F. Polizio, R. Petruzzelli, and E. Chiancone. 1991. Iron entry route in horse spleen apoferritin. *FEBS Lett.* 287:10–14.

Eggleton, R. A., and R. W. Fitzpatrick. 1988. New data and a revised structural model for ferrihydrite. *Clays and Clay Minerals.* 36:111–124.

Fleming, J., and J. G. Joshi. 1987. Ferritin: isolation of aluminum-ferritin complex from brain. *Proc. Natl. Acad. Sci. USA.* 84:7866–7870.

Ford, G. C., P. M. Harrison, D. W. Rice, J. M. A. Smith, A. Treffry, J. L. White, and J. Yariv. 1984. Ferritin: design and formation of an iron-storage molecule. *Philos. Trans. R. Soc. Lond. B. Biol. Sci.* 304: 551–565.

Harrison, P. M. 1959. The structure of ferritin and apoferritin: some preliminary x-ray data. *J. Mol. Biol.* 1:69–80.

Harrison, P. M., S. C. Andrews, P. J. Artymiuk, G. C. Ford, J. R. Guest, J. Hurzmann, D. M. Lawson, J. C. Livingstone, J. M. A. Smith, A. Treffry, and S. J. Yewdall. 1991. Probing structure-function relations in ferritin and bacterioferritin. *Adv. Inorg. Chem.* 36:449–486.

Harrison, P. M., S. C. Andrews, P. J. Artymiuk, G. C. Ford, D. M. Lawson, J. M. A. Smith, A. Treffry, and J. L. White. 1990. Ferritin. *In* Iron Transport and Storage. P. Ponka, H. M. Schulman, and R. C. Woodworth, editors. CRC Press, Boston. 81–101.

Harrison, P. M., G. C. Ford, D. W. Rice, J. M. A. Smith, A. Treffry, and J. L. White. 1986. The three-dimensional structure of apoferritin: a framework controlling ferritin's iron storage and release. *In* Frontiers in Bioinorganic Chemistry. A. V. Xavier, editor. VCH, Weinheim, Germany. 268–277.

Harrison, P. M., J. L. White, J. M. A. Smith, G. W. Farrants, G. C. Ford, D. W. Rice, J. M. Addison, and A. Treffry. 1985. Comparative aspects of ferritin structure, metal-binding and immunochemistry. *In* Proteins of Iron Storage and Transport. G. Spik, J. Montreuil, R. R. Crichton, and J. Mazurier, editors. Elsevier, Amsterdam. 67–79.

Hilty, S., B. Webb, R. B. Frankel, and G. D. Watt. 1994. Iron core formation in horse spleen ferritin: magnetic susceptibility, pH, and compositional studies. *J. Inorg. Biochem.* 56:173–185.

Jacobs, D. L., G. D. Watt, R. B. Frankel, and G. C. Papaefthymiou. 1989. Redox reactions associated with iron release from mammalian ferritin. *Biochemistry.* 28:1650–1655.

Jones, T., R. Spencer, and C. Walsh. 1978. Mechanisms and kinetics of iron release from ferritin by dihydroflavins and dihydroflavin analogs. *Biochemistry.* 17:4011–4017.

Kocherginsky, N., and Swartz, H. M. 1995. Nitroxide Spin Labels, Reactions in Biology and Chemistry. CRC Press, New York.

Lawson, D. M., P. J. Artymiuk, S. J. Yewdall, J. M. A. Smith, J. C. Livingstone, A. Treffry, A. Luzzago, S. Levi, P. Arosio, G. Cesareni, C. D. Thomas. W. V. Shaw, and P. M. Harrison. 1991. Solving the structure of human H ferritin by genetically engineering intermolecular crystal contacts. *Nature.* 349:541–544.

Massover, W. H. 1991. Dynamic stability of apoferritin: a new model to explain how impermeable reagents can reduce/capture iron within ferritin. *In* Iron Biominerals. F. B. Frankel and R. P. Blakemore, editors. Plenum Press, New York. 349–358.

Massover, W. H. 1992. Pathways for penetration of iron and negative stain across the protein shell of ferritin: ultrastructural perspectives. *In* Proc. 50th Ann. Meet. Electron Microsc. Soc. Am. G. W. Bailey, J. Bentley, and J. A. Small, editors. San Francisco Press, San Francisco. 1012–1013.

Massover, W. H. 1993. Ultrastructure of ferritin and apoferritin: a review. *Micron.* 24:389–437.

May, M. E., and W. W. Fish. 1977. The restrictive nature of apoferritin channels as measured by passive diffusion. *In* Protein of Iron Metabolism. E. B. Brown, P. Aisen, J. Fielding, and R. R. Crichton, editors. Grune & Stratton, New York. 31–38.

Moore, G. R., F. H. A. Kadir, and F. Al-Massad. 1992. Haem binding to ferritin and possible mechanisms of physiological iron uptake and release by ferritin. *J. Inorg. Biochem.* 47:175–181.

Precigoux, G., B. Yarriv, B. Gallois, A. Dautant, C. Courseille, and B. L. d'Estaintot. 1994. A crystallographic study of heme binding to ferritin. *Acta. Cryst.* D50:739–743

Price, D. J., and J. G. Joshi. 1983. Ferritin: binding of beryllium and other divalent metal ions. *J. Biol. Chem.* 258:10873–10880.

Proulx-Curry, P. M., and N. D. Chasteen. 1995. Molecular aspects of iron uptake and storage in ferritin. *Coordination Chem. Rev.* 144:347–368.

Rice, D. W., G. C. Ford, J. L. White, J. M. A. Smith, and P. M. Harrison. 1983. The spatial structure of horse spleen apoferritin. *Adv. Inorg. Biochem.* 5:39–50.

Sedmack, J. J., and S. E. Grossberg. 1977. A rapid, sensitive, and versatile assay for protein using Coomassie brilliant blue G250. *Anal. Biochem.* 79:544–552.

Smith, J. M. A., G. C. Ford, P. M. Harrison, J. Yariv, and A. J. Kaob-Gould. 1989. Molecular size and symmetry of the bacterioferritin of *Escherichia coli*: x-ray crystallographic characterization of four crystal forms. *J. Mol. Biol.* 265:465–467.

Stefanini, S., E. Chiancone, P. Vecchini, and E. Antonini. 1975. Iron incorporation and release in normal and reconstituted ferritin. *In* Proteins of Iron Storage and Transport in Biochemistry and Medicine. R. R. Crichton, editor. North Holland/Elsevier, Amsterdam. 295–302.

Stefanini, S., A. Desideri, P. Vecchini, T. Drakenberg, and E. Chiancone. 1989. Identification of the iron entry channels in apo-ferritin: chemical modification and spectroscopic studies. *Biochemistry.* 28:378–382.

Stuhrmann, H. B., J. Haas, K. Ibel, M. H. J. Koch, and R. R. Crichton. 1975. Neutron scattering of ferritin and apoferritin. *In* Proteins of Iron Storage and Transport in Biochemistry and Medicine. R. R. Crichton, editor. North Holland/Elsevier, Amsterdam. 261–266.

Stuhrmann, H. B., J. Haas, K. Ibel, M. H. J. Koch, and R. R. Crichton. 1976. Low angle neutron scattering of ferritin studies by contrast variation. *J. Mol. Biol.* 100:399–413.

Theil, E. C. 1987. Ferritin: structure, gene regulation, and cellular function in animals, plants, and microorganisms. *Annu. Rev. Biochem.* 56: 289–315.

Theil, E. C. 1989. The ferritin family of iron storage proteins. *Adv. Enzymol. Relat. Areas Mol. Biol.* 63:421–449.

Treffry, A., E. R. Bauminger, D. Hechel, N. W. Hodson, I. Nowik, S. J. Yewdall, P. M. Harrison. 1993. Defining the roles of the three-fold channels in iron uptake, iron oxidation, and iron-core formation in ferritin: a study aided by site-directed mutagenesis. *Biochem. J.* 296:721–728.

Treffry, A., and P. M. Harrison. 1984. Spectroscopic studies on the binding of iron, terbium, and zinc by apoferritin. *J. Inorg. Biochem.* 21:9–20.

Wardeska, J. G., B. Viglione, and N. D. Chasteen. 1986. Metal ion complexes of apoferritin: evidence for initial binding in the hydrophilic channels. *J. Biol. Chem.* 261:6677–6683.

Watt, G. D., R. B. Frankel, and G. C. Papaethymiou. 1985. Reduction of mammalian ferritin. *Proc. Natl. Acad. Sci. USA.* 82:3640–3643.

Watt, R. K., R. B. Frankel, and G. D. Watt. 1992. Redox reactions of apo mammalian ferritin. *Biochemistry.* 31:9673–9679.

Watt, G. D., D. Jacobs, and R. B. Frankel. 1988. Redox reactivity of bacterial and mammalian ferritin: is reductant entry into the ferritin interior a necessary step for iron release? *Proc. Natl. Acad. Sci. USA.* 85:7457–7461.

Webb, B., J. Frame, Z. Zhao, M. L. Lee, and G. D. Watt. 1994. Molecular entrapment of small molecules within the interior of horse spleen ferritin. *Arch. Biochem. Biophys.* 309:178–183.

Yang, D., and K. Nagayama. 1995. Permeation of small molecules into the cavity of ferritin as revealed by proton nuclear magnetic resonance relaxation. *Biochem. J.* 307:253–256.